

Efficient Evaluation of Reaction Integrals in the EFIE Analysis of Planar Layered Structures With Uniaxial Anisotropy

Francisco Mesa, *Member, IEEE*, Gonzalo Plaza, and Francisco Medina, *Senior Member, IEEE*

Abstract—This paper presents an efficient implementation of the electric-field integral-equation (EFIE) method to deal with planar anisotropic layered printed structures. A convenient treatment of the kernel of the integral equation gives rise to reaction integrals that only involve quasi-singularities and R^{-1} -type singularities. When the well-known Rao–Wilton–Glisson triangular basis functions are used in conjunction with the Galerkin’s method, closed-form expressions are found for the singular parts of the self-reaction integrals, as well as for the inner convolution integrals of the remaining singular/quasi-singular reaction integrals. Thus, the present procedure sets the EFIE method as a competitive alternative to other formulations.

Index Terms—Anisotropy, Dyadic Green’s function, EFIE, planar structures.

I. INTRODUCTION

THE analysis of scattering, radiation, and propagation in planar layered structures with printed conductors is often carried out by means of the mixed-potential integral-equation (MPIE) method [1]–[4]. Although a pure electric-field integral-equation (EFIE) scheme has been also used [5]–[7], the superiority of the MPIE is commonly accepted because of the scalar nature of its potentials and the lower order of the singularities involved in this method [8]. However, it was recently shown in [9] that the transverse electric-field Green’s dyadic (TEFGD) of a layered structure with uniaxial anisotropy can also be derived from two scalar potentials and that only singularities of the R^{-1} type have to be handled to solve the EFIE. Specifically, the application of potential-based techniques to deal with the R^{-3} -type singularity originally appearing in the TEFGD makes it possible to express the electric field produced by an elementary current source in terms of functions (and their derivatives) showing at most R^{-1} -type singularities. In principle, this treatment would make the EFIE method somewhat equivalent to the MPIE method, although to assure this equivalence, it should be demonstrated that the EFIE reaction integrals can be computed efficiently. This task will be the main purpose of this study. First, it will be carried out as a convenient decomposition of the TEFGD to separate the regular and nonregular (singular and

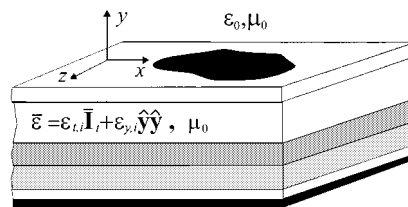


Fig. 1. Planar anisotropic layered structure under study.

quasi-singular) parts. Since the numerical computation of the reaction integrals related to the regular part of the TEFGD is rather straightforward, this paper will focus on the computation of the reaction integrals associated with the nonregular parts of the TEFGD. In this objective, part of the extensive work done in the past can be advantageously applied, although new integrals have to be treated. Thus, it has been found that the singular self-reaction double integrals can be computed by means of closed-form expressions. For the remaining nonregular reaction integrals, closed-form expressions are only found for the corresponding convolution products, although their smooth behavior allows for the use of low-order quadrature formulas to perform the exterior integral. Numerical examples will be finally shown to check the accuracy and efficiency of the present approach when applied to isotropic and anisotropic structures.

II. DECOMPOSITION OF THE TEFGD

It was shown in [9] that the spectral-domain TEFGD for a laterally open-layered structure with uniaxial anisotropy as that shown in Fig. 1 can be written as

$$\bar{\mathbf{G}}(k_\rho, \xi) = Q(k_\rho) \bar{\mathbf{I}}_t + T(k_\rho) \left[2\hat{\mathbf{k}}_\rho \hat{\mathbf{k}}_\rho - \bar{\mathbf{I}}_t \right] \quad (1)$$

where k_ρ and ξ are the radial and angular spectral variables, respectively, and $Q(k_\rho)$, $T(k_\rho)$ are radial spectral functions that can be computed starting from any of the algorithms developed in the literature, e.g., [10]–[14]. (In the following, the spectral/spatial nature of the different quantities will be apparent looking at the corresponding variables.) Each substrate of the layered medium can be uniaxial dielectric and, therefore, characterized by the following permittivity dyadic:

$$\bar{\boldsymbol{\epsilon}}_i = \epsilon_0 \left[\epsilon_{t,i} \bar{\mathbf{I}}_t + \epsilon_{y,i} \hat{\mathbf{y}} \hat{\mathbf{y}} \right] \quad (2)$$

where the symbol $\hat{\cdot}$ indicates a unit vector and $\bar{\mathbf{I}}_t = \hat{\mathbf{x}} \hat{\mathbf{x}} + \hat{\mathbf{z}} \hat{\mathbf{z}}$ is the unit transverse dyadic (subscript t will indicate in the following *transverse* to the y axis).

Manuscript received August 5, 2001. This work was supported by the Comisión Interministerial de Ciencia y Tecnología, Spain under Project TIC98-0630

F. Mesa and G. Plaza are with the Department of Applied Physics I, University of Seville, 41012 Seville, Spain (e-mail: mesa@us.es).

F. Medina is with the Department of Electronics and Electromagnetism, University of Seville, 41012 Seville, Spain (e-mail: medina@us.es).

Publisher Item Identifier 10.1109/TMTT.2002.802327.

The corresponding spatial counterpart of (1) is found to be

$$\begin{aligned} \overline{\mathbf{G}}(\mathbf{R}) &= S_0 \left\{ \overline{\mathbf{G}}(k_\rho, \xi) \right\} \\ &= S_0 \left\{ Q(k_\rho) \right\} \overline{\mathbf{I}}_t + S_2 \left\{ T(k_\rho) \right\} \left[\overline{\mathbf{I}}_t - 2\hat{\mathbf{R}}\hat{\mathbf{R}} \right] \end{aligned} \quad (3)$$

where $S_m\{\cdot\}$ stands for the Fourier–Bessel transform of m th order and $\mathbf{R} = \mathbf{r} - \mathbf{r}'$ denotes the vector from the source to the field point.

A convenient decomposition of (3) for further computational purposes requires a previous identification of the singularities and main quasi-singularities of this dyadic. This task was done in [9], which suggests for us to now write (3) as

$$\overline{\mathbf{G}}(\mathbf{R}) = \overline{\mathbf{G}}_{\text{no-reg}}(\mathbf{R}) + \overline{\mathbf{G}}_{\text{reg}}(\mathbf{R}) \quad (4)$$

where

$$\overline{\mathbf{G}}_{\text{no-reg}}(\mathbf{R}) = \overline{\mathbf{G}}_{(-1)}(\mathbf{R}) + \overline{\mathbf{G}}_{\text{elst}}(\mathbf{R}) \quad (5)$$

with

$$\begin{aligned} \overline{\mathbf{G}}_{(-1)}(\mathbf{R}) &= -\frac{j\omega\mu_0}{4\pi} \frac{\overline{\mathbf{I}}_t - 2\Gamma(\overline{\mathbf{I}}_t - \hat{\mathbf{R}}\hat{\mathbf{R}})}{R} \\ \overline{\mathbf{G}}_{\text{elst}}(\mathbf{R}) &= -\frac{1}{4\pi j\omega\epsilon_0\epsilon_{\text{eff}}} \cdot \left\{ \nabla_t \nabla_t' \frac{1}{R} - \frac{2\epsilon_{\text{eq}}}{1 + \epsilon_{\text{eq}}} \nabla_t \nabla_t' \frac{1}{\sqrt{R^2 + H_1^2}} \right\}. \end{aligned} \quad (6)$$

In this paper, $\overline{\mathbf{G}}_{(-1)}(\mathbf{R})$ will account for the R^{-1} -type singular term and $\overline{\mathbf{G}}_{\text{elst}}(\mathbf{R})$ for only the two most significant electrostatic-type terms, namely, the hypersingular R^{-3} -type term (which was also discussed in [15] in a different context) plus the quasi-singular first dipole-image term [9]. In (6) and (7), H_1 denotes the vertical distance at which the first physical dipole image is located and

$$\epsilon_{\text{eq}} = \sqrt{\epsilon_{t,N}\epsilon_{y,N}} \quad (8)$$

$$\epsilon_{\text{eff}} = \frac{1 + \epsilon_{\text{eq}}}{2} \quad (9)$$

$$\Gamma = \frac{\epsilon_{\text{eq}}(2 - \epsilon_{y,N} + \epsilon_{\text{eq}})}{8\epsilon_{\text{eff}}^2} \quad (10)$$

where subindex N denotes the layer upon which the metallization is printed.

Once the singularities and most significant quasi-singularity of the TEFGD have been properly extracted out, $\overline{\mathbf{G}}_{\text{reg}}(\mathbf{R})$ clearly shows a *smooth* although oscillatory behavior that could be eventually well fitted by a series of complex exponentials after properly applying the discrete complex-image technique (DCIT) [16], [17].

III. REACTION INTEGRALS

The solution of the EFIE by means of Galerkin's method, when using the well-known and very flexible

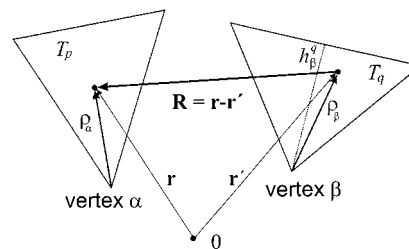


Fig. 2. Some geometrical quantities related to triangles T_p and T_q .

Rao–Wilton–Glisson (RWG) triangular basis functions [1], leads to reaction integrals of the type

$$Z_{\alpha\beta}^{pq} = \frac{1}{h_\alpha^p h_\beta^q} \int_{T_p} \boldsymbol{\rho}_\alpha(\mathbf{r}) \cdot \left[\int_{T_q} \overline{\mathbf{G}}(\mathbf{R}) \cdot \boldsymbol{\rho}_\beta(\mathbf{r}') dS' \right] dS. \quad (11)$$

(See Fig. 2 for a description of geometrical quantities involved; h_β^q is the height of triangle T_q measured from vertex β .) Considering now the decomposition of the TEFGD into its so-called regular and nonregular parts, shown in (4), (11) will be accordingly written as

$$Z_{\alpha\beta}^{pq} = Z_{\alpha\beta,\text{no-reg}}^{pq} + Z_{\alpha\beta,\text{reg}}^{pq} \quad (12)$$

Due to the smooth behavior of $\overline{\mathbf{G}}_{\text{reg}}(\mathbf{R})$, $Z_{\alpha\beta,\text{reg}}^{pq}$ double integrals are not expected to raise numerical problems, thus allowing for an accurate enough numerical integration by means of low-order quadrature formulas without much computational effort. Anyhow, if the DCIT was used to expand $\overline{\mathbf{G}}_{\text{reg}}$, the corresponding reaction integrals could be eventually computed in closed form [18].

The nonregular part of (12) can be conveniently expressed as

$$Z_{\alpha\beta,\text{no-reg}}^{pq} = \frac{1}{h_\alpha^p h_\beta^q} \left(\Omega_{\alpha\beta}^{pq} + \Upsilon_{\alpha\beta}^{pq} \right) \quad (13)$$

where $\Omega_{\alpha\beta}^{pq}$ has as kernel $\overline{\mathbf{G}}_{(-1)}(\mathbf{R})$

$$\begin{aligned} \Omega_{\alpha\beta}^{pq} &= -\frac{j\omega\mu_0}{4\pi} \int_{T_p} \boldsymbol{\rho}_\alpha(\mathbf{r}) \\ &\cdot \left[\int_{T_q} \frac{1}{R} \left[\overline{\mathbf{I}}_t - 2\Gamma(\overline{\mathbf{I}}_t - \hat{\mathbf{R}}\hat{\mathbf{R}}) \right] \cdot \boldsymbol{\rho}_\beta(\mathbf{r}') dS' \right] dS \end{aligned} \quad (14)$$

and $\Upsilon_{\alpha\beta}^{pq}$ is associated with $\overline{\mathbf{G}}_{\text{elst}}(\mathbf{R})$. The presence of the double nabla operator in (7) makes it possible to express $\Upsilon_{\alpha\beta}^{pq}$ as

$$\Upsilon_{\alpha\beta}^{pq} = - \int_{T_p} \boldsymbol{\rho}_\alpha(\mathbf{r}) \cdot \nabla_t \Phi_\beta^q(\mathbf{r}) dS \quad (15)$$

where

$$\begin{aligned} \Phi_\beta^q(\mathbf{r}) &= \frac{1}{4\pi j\omega\epsilon_0\epsilon_{\text{eff}}} \\ &\times \int_{T_q} \left[\frac{1}{R} - \frac{2\epsilon_{\text{eq}}}{1 + \epsilon_{\text{eq}}} \frac{1}{\sqrt{R^2 + H_1^2}} \right] \nabla_t' \cdot \boldsymbol{\rho}_\beta(\mathbf{r}') dS' \end{aligned} \quad (16)$$

can be seen as the electrostatic potential due to a surface charge density $(-\nabla_t \cdot \boldsymbol{\rho}_\beta / j\omega)$ and its corresponding first image. Applying now a Gauss divergence theorem (taking into account that $\nabla_t \cdot \boldsymbol{\rho}_\beta(\mathbf{r}) = 2$), (15) can be transformed into

$$\Upsilon_{\alpha\beta}^{pq} = -\frac{1}{\pi j\omega\epsilon_0\epsilon_{\text{eff}}} \cdot \left[\int_{T_p} \int_{T_q} \frac{dS dS'}{R} - \frac{2\epsilon_{\text{eq}}}{1 + \epsilon_{\text{eq}}} \int_{T_p} \int_{T_q} \frac{dS dS'}{\sqrt{R^2 + H_1^2}} \right] \quad (17)$$

in addition to other contour integrals that finally do not contribute.

Looking at (14) and (17), it can be observed that three different types of integrals have to be dealt with. Their efficient computation will be discussed in the following sections.

A. Integrals Associated to $\overline{\mathbf{G}}_{(-1)}$

In this case, the integral to be solved is shown in (14), which can be now conveniently written as

$$\Omega_{\alpha\beta}^{pq} = -\frac{j\omega\mu_0}{4\pi} I_{(-1)} \quad (18)$$

where

$$I_{(-1)} = \int_{T_p} \boldsymbol{\rho}_\alpha \cdot \left[\int_{T_q} \frac{1}{R} [(1 - 4\Gamma)\overline{\mathbf{I}}_t + 2\Gamma(\overline{\mathbf{I}}_t + \hat{\mathbf{R}}\hat{\mathbf{R}})] \cdot \boldsymbol{\rho}_\beta dS' \right] dS. \quad (19)$$

This latter integral can be expressed in terms of the auxiliary integrals I_2 and I_3 defined in [19] as

$$I_{(-1)} = (1 - 4\Gamma)I_2 + 2\Gamma I_3. \quad (20)$$

Therefore, $I_{(-1)}$ can be efficiently computed following the scheme discussed by Arcioni *et al.* [19], which made use of certain integrals previously solved in [1] and [20] or more recently in [21].

B. Integrals Associated to $\overline{\mathbf{G}}_{\text{elst}}$

Expression (17) is composed of two different integrals associated with the electrostatic-type source and first image terms of the TEFGD, respectively. This suggests to express (17) as

$$\Upsilon_{\alpha\beta}^{pq} = -\frac{1}{\pi j\omega\epsilon_0\epsilon_{\text{eff}}} \left[I_1^{(0)} + I_1^{(1)} \right] \quad (21)$$

with

$$I_1^{(0)} = \int_{T_p} \int_{T_q} \frac{dS dS'}{R} = \int_{T_p} I_4^{(0)}(\mathbf{r}) dS \quad (22)$$

$$I_1^{(1)} = \int_{T_p} \int_{T_q} \frac{dS dS'}{\sqrt{R^2 + H_1^2}} = \int_{T_p} I_4^{(1)}(\mathbf{r}) dS. \quad (23)$$

Integral $I_1^{(0)}$ can be computed following the scheme given in [19], where a complete closed-form expression is given for the particular case $T_p = T_q$. When $T_p \neq T_q$, the smooth behavior of the closed-form expression found for $I_4^{(0)}$ (see further) allows for an accurate numerical integration over the triangle using a

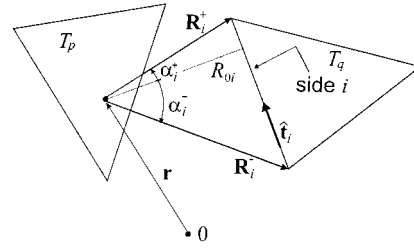


Fig. 3. Geometrical quantities associated with integral $I_4^{(1)}$.

seven-point integration formula [20] (at least three significant digits were found for the worst numerical case involving adjacent triangles; a lower order quadrature formula can be used for distant triangles).

For double integral $I_1^{(1)}$, no closed-form expression was found by the authors for any case. Nevertheless, the following closed-form expression was obtained for the inner convolution integral $I_4^{(1)}$:

$$I_4^{(1)} = \sum_{i=1}^3 \left[\Lambda(\alpha_i^+) - \Lambda(\alpha_i^-) \right] \quad (24)$$

where (according to the notation given in Fig. 3) the summation is extended to the three sides of the triangle involved and

$$\Lambda(\alpha_i) = -H_1 \alpha_i + \frac{R_{oi}}{2} \ln \left(\frac{\sqrt{d_i^2 - H_1^2 \sin^2 \alpha_i} + R_{oi} \sin \alpha_i}{\sqrt{d_i^2 - H_1^2 \sin^2 \alpha_i} - R_{oi} \sin \alpha_i} \right) + H_1 \arcsin \left(\frac{H_1}{d_i} \sin \alpha_i \right) \quad (25)$$

with

$$\sin \alpha_i^\pm = \frac{\mathbf{R}_i^\pm \cdot \hat{\mathbf{t}}_i}{R_i^\pm} \quad d_i = \sqrt{R_{oi}^2 + H_1^2}.$$

(Clearly, $I_4^{(0)}$ can be directly computed from the above expressions after taking $H_1 = 0$.) The smooth behavior of $I_4^{(1)}$ again causes that integral (23) can be efficiently computed with a low-order integration formula for both coincident and noncoincident triangles.

IV. NUMERICAL RESULTS

The above scheme has been used to develop a computer code to deal with general planar anisotropic layered structures. This code has been checked with previously published data for different isotropic/anisotropic structures, giving satisfactory results.

As a first example, Table I shows our results in comparison with those in [22] for the resonant frequency f_r of the fundamental resonant mode of a circular disk. The numerical data provided in [22] (f_r^{num} in Table I) were computed by means of an EFIE method solved in the spectral domain by using Chebyshev-polynomials full-domain basis functions [22]. This method was specifically designed to deal with circular resonators and has proven to be very accurate. The remaining data in Table I were obtained from the frequency associated with the dip in the reflection coefficient when the resonator is

TABLE I

RESONANT FREQUENCY OF THE FUNDAMENTAL RESONANT MODE OF A CIRCULAR DISK WITH RADIUS = a PRINTED ON A GROUNDED ISOTROPIC DIELECTRIC SUBSTRATE: $\epsilon_r = 2.43$, $h = 0.49$ mm. THE NUMERICAL RESULTS OF THIS PAPER (f_r^{TW}) ARE COMPARED WITH THE FOLLOWING DATA PROVIDED IN [22]: EXPERIMENTAL DATA (f_r^{EXP}), NUMERICAL DATA (f_r^{NUM}), AND DATA OBTAINED WITH ELECTROMAGNETIC SIMULATOR ENSEMBLE (f_r^{ENS})

| a/h | f_r^{EXP} | f_r^{NUM} | f_r^{ENS} | f_r^{TW} |
|-------|-------------|-------------|-------------|------------|
| 8.08 | 13.1 | 13.2 | 13.4 | 13.1 |
| 12.02 | 8.96 | 9.07 | 9.17 | 9.03 |
| 16.33 | 6.81 | 6.76 | 6.83 | 6.75 |
| 20.33 | 5.47 | 5.46 | 5.53 | 5.46 |

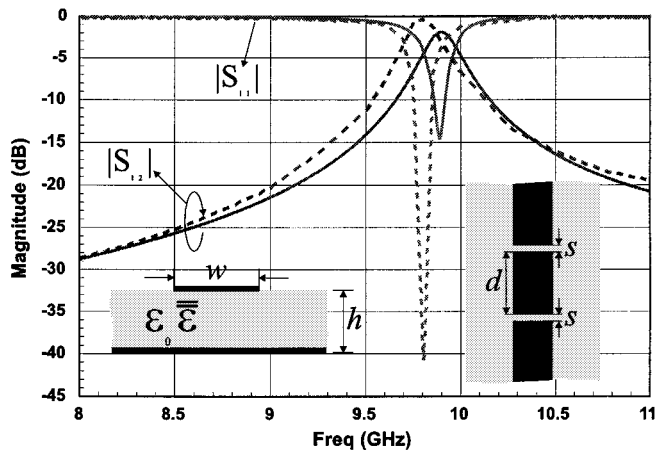


Fig. 4. Return and insertion losses of coupled resonator bandpass filter on anisotropic Epsilam-10: $\epsilon_x = 13$, $\epsilon_y = 10.3$. Solid lines: our results. Dashed lines: results by Drake *et al.* [23].

capacitively feed by means of a $50\text{-}\Omega$ microstrip line. It can be seen that the agreement of our results with the numerical ones in [22] is very good. A good agreement with experimental and “Ensemble” data is also observed.

A second example of comparison with an anisotropic structure is shown in Fig. 4, which shows the scattering parameters of a microstrip bandpass filter containing two microstrip gap discontinuities when the substrate is anisotropic Epsilam-10 [23]. Our data agree reasonably well with those reported in [23] (the error of 1% in the resonant frequency can be attributed to the boxed nature of the structure analyzed in [23]). To give an idea of the computational effort of the present formulation, the CPU time required by a PC Pentium 233 MHz (64 MB of RAM) for filling the Galerkin matrix in this particular structure has taken approximately 180 s when a large number of RWG basis functions (850) are used. For practical purposes, good enough results may be obtained with less basis functions.

V. CONCLUSIONS

An efficient scheme to compute the reaction integrals involved in the application of Galerkin’s method to solve the EFIE of planar anisotropic layered printed structures has been presented in this paper. Our proposed EFIE scheme makes use of a convenient treatment of the singularities and quasi-singularities of the TEFGD that leads to reaction integrals similar to

those found in the MPIE method. Closed-form expressions can be used to compute the singular self-reaction double integrals. The inner convolution integrals of the remaining singular and quasi-singular reaction integrals can be also obtained in closed form. As a consequence, the present formulation of the EFIE makes this method as accurate and efficient as some other alternative methods for this kind of problem.

REFERENCES

- [1] S. M. Rao, D. R. Wilton, and A. W. Glisson, “Electromagnetic scattering by surfaces of arbitrary shape,” *IEEE Trans. Antennas Propagat.*, vol. AP-30, pp. 409–418, May 1982.
- [2] K. A. Michalski and D. Zheng, “Electromagnetic scattering and radiation by surfaces of arbitrary shape in layered media,” *IEEE Trans. Antennas Propagat.*, vol. 38, pp. 335–352, Mar. 1997.
- [3] J. Sercu, N. Faché, F. Libbrecht, and P. Lagase, “Mixed potential integral equation technique for hybrid microstrip-slotline multilayered circuits using a mixed rectangular-triangular mesh,” *IEEE Trans. Microwave Theory Tech.*, vol. 43, pp. 1162–1172, May 1995.
- [4] R. Bunge and F. Arndt, “Efficient MPIE approach for the analysis of three-dimensional microstrip structures in layered media,” *IEEE Trans. Microwave Theory Tech.*, vol. 45, pp. 1141–1153, Aug. 1997.
- [5] P. B. Katehi and N. G. Alexopoulos, “Frequency-dependent characteristics of microstrip discontinuities in millimeter-wave integrated circuits,” *IEEE Trans. Microwave Theory Tech.*, vol. MTT-33, pp. 1029–1035, Oct. 1985.
- [6] J. Sercu, N. Faché, F. Libbrecht, and D. De Zutter, “Full-wave space-domain analysis of open microstrip discontinuities including the singular current-edge behavior,” *IEEE Trans. Microwave Theory Tech.*, vol. 41, pp. 1581–1588, Sept. 1993.
- [7] A. Toscano and L. Vegni, “Spectral dyadic Green’s function formulation for planar integrated structures with a grounded chiral slab,” *J. Electromagn. Waves Applicat.*, vol. 6, no. 5–6, pp. 751–769, 1992.
- [8] D. C. Chang and J. X. Zheng, “Electromagnetic modeling of passive circuits elements in MMIC,” *IEEE Trans. Microwave Theory Tech.*, vol. 40, pp. 1741–1747, Sept. 1992.
- [9] G. Plaza, F. Mesa, and F. Medina, “Treatment of singularities and quasi-static terms in the EFIE analysis of planar structures,” *IEEE Trans. Antennas Propagat.*, vol. 40, pp. 485–491, Apr. 2002.
- [10] C. M. Krowne, “Fourier transform matrix method of finding propagation characteristics of complex anisotropic layered media,” *IEEE Trans. Microwave Theory Tech.*, vol. MTT-32, pp. 1617–1625, Dec. 1984.
- [11] R. Marqués and M. Horno, “On the spectral dyadic Green’s function for stratified linear media,” *Proc. Inst. Elect. Eng.*, pt. H, vol. 134, pp. 241–248, June 1987.
- [12] L. Beyne and D. De Zutter, “Green’s function for layered lossy media with special application to microstrip antennas,” *IEEE Trans. Microwave Theory Tech.*, vol. 36, pp. 875–881, Apr. 1988.
- [13] F. Mesa, R. Marqués, and M. Horno, “A general algorithm for computing the bidimensional spectral Green’s dyad in multilayered complex bianisotropic media: The equivalent boundary method,” *IEEE Trans. Microwave Theory Tech.*, vol. 39, pp. 1640–1649, Sept. 1991.
- [14] K. A. Michalski and J. R. Mosig, “Multilayered media Green’s functions in integral equations formulations,” *IEEE Trans. Antennas Propagat.*, vol. 45, pp. 508–519, Mar. 1997.
- [15] M. Bressan and G. Conciauro, “Singularity extraction from the electric Green’s function for a spherical resonator,” *IEEE Trans. Microwave Theory Tech.*, vol. MTT-33, pp. 407–414, May 1985.
- [16] Y. L. Chow, J. J. Yang, and G. Y. Howard, “A closed-form spatial Green’s function for the thick microstrip substrate,” *IEEE Trans. Microwave Theory Tech.*, vol. 39, pp. 588–592, Mar. 1991.
- [17] R. A. Kipp and C. H. Chan, “Complex image method for sources in bounded regions of multilayer structures,” *IEEE Trans. Microwave Theory Tech.*, vol. 42, pp. 860–865, May 1994.
- [18] L. Alatan, M. I. Aksun, K. Mahadevan, and M. T. Birand, “Analytical evaluation of the MoM matrix elements,” *IEEE Trans. Microwave Theory Tech.*, vol. 44, pp. 519–525, Apr. 1996.
- [19] P. Arcioni, M. Bressan, and L. Perregrini, “On the evaluation of the double surface integrals arising in the application of the boundary integral method to 3-D problems,” *IEEE Trans. Microwave Theory Tech.*, vol. 45, pp. 436–439, Mar. 1997.
- [20] R. D. Graglia, “On the numerical integration of the linear shape function times the 3-D Green’s functions or its gradient on a plane triangle,” *IEEE Trans. Antennas Propagat.*, vol. 41, pp. 1448–1455, Oct. 1993.

- [21] L. Rossi and P. J. Cullen, "On the fully numerical evaluation of the linear-shape function times the 3-D Green's function on a plane triangle," *IEEE Trans. Microwave Theory Tech.*, vol. 47, pp. 398–402, Apr. 1999.
- [22] V. Losada, R. R. Boix, and M. Horno, "Resonant modes of circular microstrip patches in multilayered structures," *IEEE Trans. Microwave Theory Tech.*, vol. 47, pp. 488–498, Apr. 1999.
- [23] E. Drake, R. R. Boix, M. Horno, and T. K. Sarkar, "Effect of substrate dielectric anisotropy on the frequency behavior of microstrip circuits," *IEEE Trans. Microwave Theory Tech.*, vol. 48, pp. 1394–1403, Aug. 2000.



Gonzalo Plaza was born in Cádiz, Spain, in November 1960. He received the Licenciado and Doctor degrees in physics from the University of Seville, Seville, Spain, in 1986 and 1995, respectively.

He is currently an Associate Professor in the Department of Applied Physics I, University of Seville. His research interest focuses on electromagnetic propagation in planar lines with complex media.



Francisco Mesa (M'94) was born in Cádiz, Spain, on April 1965. He received the Licenciado and Doctor degrees from the University of Seville, Seville, Spain, in 1989 and 1991, respectively, both in physics.

He is currently an Associate Professor in the Department of Applied Physics I, University of Seville. His research interest focuses on electromagnetic propagation/radiation in planar lines with general anisotropic materials.



Francisco Medina (M'90–SM'01) was born in Puerto Real, Cádiz, Spain, in November 1960. He received the Licenciado and Doctor degrees from the University of Seville, Seville, Spain, in 1983 and 1987, respectively, both in physics.

From 1986 to 1987, he spent the academic year with the Laboratoire de Microondes de l'ENSEEIH, Toulouse, France. From 1985 to 1989, he was a Profesor Ayudante (Assistant Professor) with the Department of Electronics and Electromagnetism, University of Seville, and since 1990, he has been a Profesor

Titular (Associate Professor) of electromagnetism. He is also currently Head of the Microwaves Group, University of Seville. His research interest includes analytical and numerical methods for guidance, resonant and radiating structures, passive planar circuits, and the influence on these circuits of anisotropic materials.

Dr. Medina was a member of both the Technical Program Committee (TPC) of the 23rd European Microwave Conference, Madrid, Spain, 1993, and the TPC of ISRAMT'99, Malaga, Spain. He is on the Editorial Board of the IEEE TRANSACTIONS ON MICROWAVE THEORY AND TECHNIQUES. He has been a reviewer for other IEEE and Institution of Electrical Engineers (IEE), U.K., publications.